

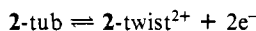
The dicationic species of the dicobalt complex **2** is also obtained in quantitative yields by chemical oxidation of **2** with  $\text{AgPF}_6$  in diethyl ether. Despite numerous attempts we were unable to grow crystals of  $2^{2+}$  suitable for X-ray structure determination. However, the low-temperature  $^1\text{H}$  NMR spectrum of this complex in  $\text{CD}_3\text{NO}_2$  shows four signal groups,<sup>7</sup> with the same chemical shift and splitting patterns, corresponding to four nonequivalent protons of cot, as for the dirhodium complex  $3^{2+}$ . It seems reasonable therefore to suggest a structure for the dicobalt species similar to that in Figure 1.

The electrochemistry of  $2^{2+}$  and  $3^{2+}$  is complementary to that of the neutral complexes. The dicobalt complex shows the same quasi-reversible wave observed for the electrochemical oxidation product of **2**. The dirhodium dication, which is virtually insoluble in  $\text{CH}_2\text{Cl}_2$ , is reduced in nitromethane irreversibly at  $-0.30$  V, with a coupled irreversible oxidation at  $+0.35$  V.

An intriguing question involves the difference in apparent electron-transfer rates of  $2^{0/2+}$  and  $3^{0/2+}$ , the heterogenous standard electron-transfer rate of **2** (ca.  $6 \times 10^{-3}$  cm/s by digital simulation of CV curves) being about 5 orders of magnitude larger than that predicted from the very large CV peak separations of **3**. The voltammetry can be best explained if the structural rearrangements involving **3** and  $3^{2+}$  occur subsequent to (not concerted with) the electron-transfer steps. Thus, the oxidation/reduction peaks of  $(\text{CpRh})_2(\text{cot})$  do not form a quasi-reversible couple; rather each peak represents an electron-transfer reaction followed by a chemical reaction (the structural rearrangement). For example, reduction of the cot-twisted dication,  $3\text{-twist}^{2+}$ , involves initial formation of a neutral cot-twisted complex (the bottom line of Scheme I) followed by rearrangement to the neutral cot-tub form **3-tub**. In this regard, the structural rearrangements are viewed as isomerizations coupled to the electron transfer (EEC mechanism, Scheme I).<sup>8</sup>

This interpretation suggests that it should be possible to find experimental conditions in which the tub form of  $3^{2+}$  or the twisted form of **3** can be observed prior to rearrangement. Indeed rapid CV scans of  $3\text{-twist}^{2+}$  in acetone give a reversible reduction at  $E^\circ = -0.11$  V, suggesting that the neutral twisted form **3-twist** has a finite lifetime in this solvent.

The quasi-reversibility of  $2^{0/2+}$  implies that interconversion of the dicobalt tub and twisted forms occurs rapidly during the electron-transfer process:



A final point is that both  $2^{2+}$  and  $3^{2+}$  are fluxional at elevated temperatures. At  $80^\circ\text{C}$  the four cot resonances of  $2^{2+}$  and  $3^{2+}$  merge into a broad singlet at 4.8 and 5.8 ppm, respectively. These compounds have promise as models with which to probe the redox-induced mobility of two or more metals bonded to polyolefinic hydrocarbons.

**Acknowledgment.** This work was generously supported by the National Science Foundation (CHE-8004242 and 8303974), which also provided funds to the University of Delaware for the purchase of the diffractometer. We gratefully acknowledge loan of rhodium salts from the Matthey Bishop Co. and a sample of **3** from Dr. A. Salzer.

(7)  $^1\text{H}$  NMR data:  $2^{2+}$  in  $\text{CD}_3\text{NO}_2/(\text{CD}_3)_2\text{CO}$  (2:1) at 213 K,  $\delta$  7.8 (t, 2 H, H8), 6.3 (t, 2 H, H7), 5.4 (d, 2 H, H6), 4.9 (d, 2 H, H9), 1.5 (s, 30 H, Me Cp);  $3^{2+}$  in  $\text{CD}_3\text{NO}_2$  at 243 K,  $\delta$  7.37 (t, 2 H, H8), 5.31 (t, 2 H, H7), 3.56 (d, 2 H, H6), 3.05 (d, 2 H, H9), 6.05 (s, 10 H, H Cp) ppm.

(8) This analysis is made more complicated by the fact that these are overall two-electron processes, and the structural rearrangement might possibly come after the first electron transfer in an ECE-type process.

**Supplementary Material Available:** Details of electrochemical measurements, complete listings of atomic coordinates, anisotropic thermal parameters, bond lengths and angles, hydrogen atom coordinates, and structure factor tables (14 pages). Ordering information is given on any current masthead page.

### Direct Determination of Fe-C Bond Lengths in Iron(II) and Iron(III) Cyanide Solutions Using EXAFS Spectroelectrochemistry

Doris A. Smith, M. J. Heeg, William R. Heineman, and R. C. Elder\*

Department of Chemistry, University of Cincinnati  
Cincinnati, Ohio 45221

Received January 30, 1984

We describe the development and implementation of EXAFS spectroelectrochemistry (extended X-ray absorption fine structure spectroelectrochemistry), a new technique that permits determination of local structure in species that are electrochemically generated and maintained. The ability to determine the oxidation-state dependence of metal-ligand bond lengths in solution species is desirable for the evaluation and further development of electron-transfer theories.<sup>1-3</sup> In addition, this methodology can be used to structurally characterize biological materials that normally are unstable to reduction or oxidation in an X-ray beam.<sup>4</sup> We report here experiments with the ferricyanide/ferrocyanide couple leading to the first direct, solution determination of the  $\text{Fe}^{\text{III}}\text{-C}$  and  $\text{Fe}^{\text{II}}\text{-C}$  bond distances.

The electrochemical cell used must allow X-rays to pass through the sample while having the capability for rapid and exhaustive electrolysis. A modified version of the optically transparent, thin-layer electrochemical cell<sup>5</sup> works satisfactorily. The electrolysis region measures  $38 \times 14 \times 1$  mm and the electrolysis volume is ca. 500  $\mu\text{L}$ . The working electrode consists of three layers of 100 lines per in. gold minigrad (Buckbee-Mears Co.) that lie parallel to the cell windows. Platinum wire auxiliary and  $\text{Ag}/\text{Ag}^+$  reference electrodes are inserted in the filling ports. All electrochemical procedures were performed with a CV-27 Voltammograph (Bioanalytical Systems, Inc.). Ferricyanide solutions were prepared as 10 mM solutions of  $\text{K}_3\text{Fe}(\text{CN})_6$  in deionized, organic-free water (Sybron/Barnstead). Ferrocyanide solutions were generated by electrochemical reduction of the ferricyanide solutions. Either sodium acetate or lithium acetate was added at a concentration of 1 M as the supporting electrolyte in all experiments. Electrolysis of 10 mM ferricyanide solution was 95% complete in 30 min when the cell potential was maintained at  $-200$  mV for reduction to the ferrocyanide complex or in 20 min at  $+500$  mV for reoxidation to ferricyanide.

X-ray absorption spectra about the iron K edge (6.6 to 8.1 keV) were recorded at the Stanford Synchrotron Radiation Laboratory (SSRL). Data were recorded in the fluorescence mode. Iron K edge spectra were converted to electron volts by a single-point calibration based on the  $L_{\text{III}}$  edge of  $\text{Eu}_2(\text{CO}_3)_3$  whose spectrum was recorded simultaneously. Changes that occur in the iron K edge region of the absorption spectrum upon reduction of  $[\text{Fe}(\text{CN})_6]^{3-}$  to  $[\text{Fe}(\text{CN})_6]^{4-}$  clearly indicate that reduction has taken place. The K edge region of each spectrum is dominated by an intense absorption peak, which can be attributed to an allowed  $1s \rightarrow 4p$  transition.<sup>6</sup> This transition shifts to lower energy and

(1) Sutin, N. *Prog. Inorg. Chem.* **1983**, *30*, 441-498.

(2) Endicott, J. *Prog. Inorg. Chem.* **1983**, *30*, 141-187.

(3) Creutz, C. *Prog. Inorg. Chem.* **1983**, *30*, 1-73.

(4) Chance, B.; Angiolillo, P.; Yang, E. D.; Powers, L. *FEBS Lett.* **1980**, *112*, 178.

(5) Anderson, C. W.; Halsall H. B.; Heineman, W. R. *Anal. Biochem.* **1979**, *93*, 366-372.

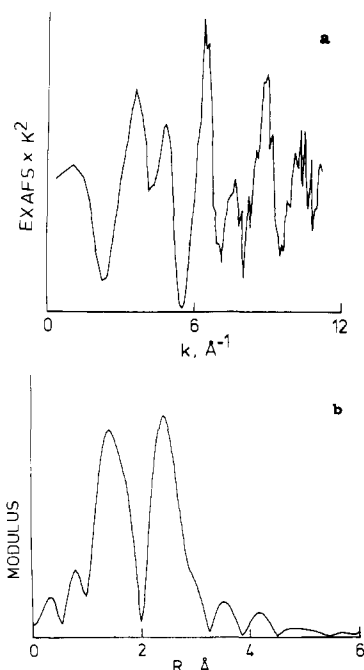


**Figure 1.** EXAFS data for electrochemically generated 10 mM  $[\text{Fe}(\text{CN})_6]^{4-}$  solution: (a) EXAFS spectrum after background subtraction and multiplication by  $k^2$ , (b) Fourier transformation of weighted EXAFS spectrum.

increases significantly in absorptivity upon reduction to the Fe(II) complex. The energies of the inflection points are  $\text{K}_3\text{Fe}(\text{CN})_6$  solid, 7127.77 (2) eV; 10 mM  $[\text{Fe}(\text{CN})_6]^{3-}$  solution, 7127.60 (7) eV;  $\text{K}_4\text{Fe}(\text{CN})_6 \cdot 2\text{H}_2\text{O}$  solid, 7126.82 (11) eV; 10 mM  $[\text{Fe}(\text{CN})_6]^{4-}$  solution, 7126.98 (4) eV, where the number in parentheses is the estimated error in the last digit. Ten EXAFS spectra were recorded and averaged for each oxidation state. The EXAFS was extracted<sup>7</sup> from the total absorption spectrum by use of a cubic spline routine, and the EXAFS component due to the carbon atoms was isolated by Fourier filtering with a window of 1.0–2.0 Å in distance ( $R$ ) space. Phase shift and amplitude parameters, obtained empirically from fits to  $\text{K}_3\text{Fe}(\text{CN})_6$  or  $\text{K}_4\text{Fe}(\text{CN})_6 \cdot 2\text{H}_2\text{O}$  solids, were used to fit data for the ferricyanide and ferrocyanide solutions over a  $k$  range of 4–10  $\text{Å}^{-1}$ .

The extracted EXAFS (multiplied by  $k^2$ ) is shown in Figure 1a for the ferrocyanide species. The complex EXAFS pattern displays a beat phenomenon arising from summation of sine waves due to backscattering contributions from carbon and nitrogen atoms where the large contribution from the latter results from the colinearity effect.<sup>8</sup> The Fourier transform of the EXAFS data into  $R$  space, illustrated in Figure 1b, displays two major peaks with the first (1–2 Å) due to carbon atoms and the second (2–3 Å) due to nitrogen atoms.

The results of single-shell fits using parameters from  $\text{K}_3\text{Fe}(\text{CN})_6$  solid are, for Fe(II),  $d = 1.97$  Å and  $N_C = 7.4$ , for Fe(III),  $d = 1.94$  Å and  $N_C = 6.8$ . Since coordination numbers ( $N_C$ ) normally are determined to only 20% accuracy by EXAFS analysis, the  $N_C$  values are indistinguishable from those of a compound having coordination number of 6. On reduction from Fe(III) to Fe(II), the Fe–C bond length increases by 0.03 Å. This is the first direct observation of these bond-length changes<sup>9</sup> for the solution species. In the past, the evaluation of electron-transfer theories has depended on the use of crystallographic bond distances, which can vary over a wide range for a single oxidation state due to differences in counterion and degree of hydration. For the ferricyanide/ferrocyanide system, the variation in crystallographic bond

lengths within the Fe(II) species<sup>10–15</sup> (10 Fe(II)–C bonds, max = 1.956, min = 1.896, mean = 1.914 (17) Å) and also for the Fe(III) moieties<sup>16–20</sup> (16 Fe(III)–C bonds, max = 1.945, min = 1.910, mean = 1.929 (9) Å) obscures the oxidation-state dependence in the Fe–C bond distance, so determination of the solution-phase bond lengths is highly desirable.

**Acknowledgment.** We thank the University of Cincinnati Research Council and N.S.F. (PCM8023743) for support. D.A.S. acknowledges support by the University of Cincinnati Neff Scholarship. We thank Dr. Jon Doi and M. K. Eidsness for aid in data collection and helpful discussions. X-ray spectra were recorded at SSRL, which is operated by the Department of Energy.

(10) Tullberg, A.; Vannerberg, N.-G. *Acta Chem. Scand., Ser. A* **1974**, *A28*, 551–562.

(11) Graveriau, P.; Garnier, E.; Hardy, A. *Acta Crystallogr., Sect. B* **1979**, *B35*, 2843–2848.

(12) Morosin, B. *Acta Crystallogr., Sect. B* **1978**, *B34*, 3730–3731.

(13) Taylor, J. C.; Mueller, M. H.; Hitterman, R. L. *Acta Crystallogr., Sect. A* **1970**, *A26*, 559–567.

(14) Beall, G. W.; Mullica, D. F.; Milligan, W. O.; Korp, J.; Bernal, I. *Acta Crystallogr., Sect. B* **1978**, *B34*, 1446–1449.

(15) Mullica, D. F.; Milligan, W. O.; Oliver, J. D. *Inorg. Nucl. Chem. Lett.* **1979**, *15*, 1–5.

(16) Mullica, D. F.; Milligan, W. O.; Garnier, R. L. *Acta Crystallogr., Sect. B* **1980**, *B36*, 2561–2564.

(17) Figgis, B. N.; Skelton, B. W.; White, A. H. *Aust. J. Chem.* **1978**, *31*, 1195–1199.

(18) Fletcher, S. R.; Gibb, T. C. *J. Chem. Soc., Dalton Trans.* **1977**, 309–316.

(19) Beall, G. W.; Milligan, W. O.; Korp, J.; Bernal, I.; McMullan, R. K. *Inorg. Chem.* **1977**, *16*, 207–209.

(20) Swanson, B. I.; Ryan, R. R. *Inorg. Chem.* **1973**, *12*, 283–286.

## Directed Cleavage of Carbon–Carbon Bonds by Transition Metals: The $\alpha$ -Bonds of Ketones

J. William Suggs\* and Chul-Ho Jun

Department of Chemistry, Brown University  
Providence, Rhode Island 02912

Received January 3, 1984

Recently, remarkable progress has been made in the activation of carbon–hydrogen bonds by homogeneous metal complexes.<sup>1</sup> Less is known about the activation of simple, unstrained carbon–carbon bonds by soluble metal species.<sup>2</sup> Two factors would seem to disfavor C–C activation. The first is accessibility. While spherical species such as  $\text{Fe}^+$  (in the gas phase)<sup>3</sup> or  $\text{H}^+$  (in superacids)<sup>4</sup> can react preferentially with hydrocarbon C–C framework bonds, nonspherical reactive intermediates (such as  $\text{CH}_2$ ) normally react with the peripheral C–H bonds. Thus, any sterically demanding species reactive enough to insert into a C–C bond will probably be intercepted by C–H bonds.<sup>5</sup> The second

(1) Watson, P. L. *J. Am. Chem. Soc.* **1983**, *105*, 6491–6493. Jones, W. D.; Feher, F. J. *Organometallics* **1983**, *2*, 562–563. Crabtree, R. H.; Mellea, M. F.; Mihelcic, J. M.; Quirk, J. M. *J. Am. Chem. Soc.* **1982**, *104*, 107–113. Janowicz, A. H.; Bergman, R. G. *Ibid.* **1982**, *104*, 352–354. Hoyano, J. K.; Graham, W. A. G. *Ibid.* **1982**, *104*, 3723–3725. Baudry, D.; Ephritikhine, M.; Felkin, H. *J. Chem. Soc., Chem. Commun.* **1980**, 1243–1244. Parshall, G. W. *Catalysis* **1977**, *1*, 335.

(2) Favero, G.; Morvillo, A.; Turco, A. *J. Organomet. Chem.* **1983**, *241*, 251–257. Ozawa, F.; Iri, K.; A. *Chem. Lett.* **1982**, 1707–1710. Bishop, K. C., III *Chem. Rev.* **1976**, *76*, 461–486. Hoberg, H.; Herrera, A. *Angew. Chem., Int. Ed. Engl.* **1981**, *20*, 876–877. Donaldson, W. A.; Hughes, R. P. *J. Am. Chem. Soc.* **1982**, *104*, 4846–4859. Burton, J. T.; Puddephatt, R. J. *Organometallics* **1983**, *2*, 1487–1494.

(3) Burnier, R. C.; Byrd, G. D.; Freiser, B. S. *J. Am. Chem. Soc.* **1981**, *103*, 4360–4367; Byrd, G. D.; Burnier, R. C.; Freiser, B. S. *Ibid.* **1982**, *104*, 3565–3569. Armentrout, P. B.; Halle, L. F.; Beauchamp, J. L. *Ibid.* **1981**, *103*, 6501–6502.

(4) Olah, G. A. *Angew. Chem., Int. Ed. Engl.* **1973**, *12*, 173–212.

(5) This may not be an insurmountable problem with metal complexes. Since alkyl metal hydrides tend to be less stable than metal dialkyls, conditions may exist under which products from rapid reversible C–H activation are slowly drained off into metal dialkyls formed essentially irreversibly.

(6) Shulman, R. G.; Yafet, Y.; Eisenberger, P.; Blumberg, W. E. *Proc. Nat. Acad. Sci. U.S.A.* **1976**, *73*, 1384–1388.

(7) Cramer, S. P.; Hodgson, K. O. *Prog. Inorg. Chem.* **1979**, *25*, 1–39.

(8) Teo, B. K. *J. Am. Chem. Soc.* **1981**, *103*, 3990–4001.

(9) On the basis of this and other EXAFS studies of single-shell complexes, we estimate the error in the difference to be 0.01 Å.